

Z. GRONOSTAJSKI*, M. HAWRYLUK*, R. KUZIAK**, K. RADWAŃSKI**, T. SKUBISZEWSKI*, M. ZWIERZCHOWSKI*

THE EQUAL CHANNEL ANGULAR EXTRUSION PROCESS OF MULTIPHASE HIGH STRENGTH ALUMINIUM BRONZE

PROCES RÓWNOKANAŁOWEGO WYCISKANIA KĄTOWEGO WYSOKOWYTRZYMAŁYCH WIELOFAZOWYCH BRĄZÓW ALUMINIOWYCH

The aim of the research was to determine the deformation condition of ECAP process of multiphase high strength aluminium bronze BA1032. The studies have indicated that it is possible to deform multiphase aluminium bronze BA1032 in the ECAP process at a temperature of 400°C and die angle $\Phi = 110^\circ$. The deformation of the bronzes at lower temperatures encounters some difficulties – cracks appear which make repeated ECAP impossible. The cracks appear on the top surface of the samples where it contacts the surface of the outlet channel. FEM simulations show that the largest plastic strains occur in this area. The proposed ECAP method of large plastic deformations as applied to the investigated aluminium bronzes makes it possible to obtain very strong refinement especially of eutectoid $\alpha + \gamma_2$.

Keywords: aluminium bronzes, ECAP, strain, microstructure, grain size

Celem pracy było określenie warunków odkształcania w procesie ECAP wysokowytrzymałych wielofazowych brązów aluminiowych. Przeprowadzone badania wskazują na możliwość odkształcania wielofazowych brązów aluminiowych w tym procesie w temperaturze 400°C dla kąta matrycy $\Phi = 110^\circ$. Pewne trudności sprawia odkształcanie brązu w niższych temperaturach, gdyż pojawiają się wówczas pęknięcia, które uniemożliwiają prowadzenie procesu wielokrotnego przeciskania próbek przez kanał kątowy. Pęknięcia pojawiają się na górnej powierzchni próbek w miejscu kontaktu z powierzchnią kanału wyjściowego. Jak wykazuje symulacje MES w miejscu tym występują największe odkształcenia plastyczne. Zastosowana metoda dużych odkształceń plastycznych ECAP w przypadku badanych brązów aluminiowych pozwala uzyskać bardzo silne rozdrobnienie głównie eutektoidu $\alpha + \gamma_2$.

1. Introduction

Aluminium bronzes are characterized by good mechanical properties at room temperature and at elevated temperature and by abrasion resistance and corrosion resistance (high in comparison with that of other copper alloys, owing to passivation and the formation of an Al_2O_3 coating on their surface) [1, 2].

Single-phase aluminium bronzes with an aluminium content of 4-6% can be subjected to both cold and hot plastic working whereas multiphase aluminium can be only hot deformed due to very large strength [3-5].

Aluminium bronzes are used for parts intended for the chemical industry, for power and electrical equipment, coins, sliding contacts, parts of bearings, shafts, bolts, sieves and components working in seawater (because of their high resistance to the corrosive action of

seawater), such as screw propellers, casings, pump parts and ship fittings.

The analysis of multiphase aluminium bronzes BA1032 and BA1054, in the form of bars, clearly shows that after hot extrusion the product microstructure is highly heterogeneous along its length. This is one of the main problem the Hutmen S.A. Company, the largest producer of aluminium bronzes, struggle with.

This considerable heterogeneity of the structure as regards the distribution and size of grains along the product length is caused by the variation in the temperature of the charge in the recipient sleeve during the process. The initial volume of the outflowing material was deformed at a temperature higher by about 100-150°C than the temperature at which the final charge volume was deformed. As a result, the grains of the aluminium bronze microstructure in the different sections of the bar under-

* WROCLAW UNIVERSITY OF TECHNOLOGY, INSTITUTE OF PRODUCTION ENGINEERING AND AUTOMATION, 50-371 WROCLAW, 5 IGNACEGO LUKASIEWICZA STR., POLAND

** INSTITUTE FOR FERROUS METALLURGY, 44-100 GLIWICE, 12-14 K. MIARKI, POLAND

went recrystallization at different temperatures. The final volume of the deformed ingot was worked at a temperature lower by about 150-200°C whereby recrystallization taking place at the lower thermal gradient of the charge and the tools did not result in substantial grain growth [5, 6].

The analysis has confirmed that the charge temperature has the most critical effect on the size and distribution of grains in the microstructure of the plastically deformed material. The tests have shown that the aluminium bronzes, especially BA1032, are very sensitive to deformation temperature. As a result, an apparently correct extrusion process may produce completely different microstructures, which may affect the final properties of the product.

ECAP (Equal Channel Angular Pressing) is a novel method to get a sub-micron grain structure in metallic and intermetallic materials through intense plastic deformation by simple shear. In this method, a material is cyclically pushed through a die with two intersecting channels and has a simple shear deformation. The amount of plastic strain in one pass depends mainly on the channel angle. Invented by Segal [7] the method has been proven to be very effective in producing an ultra-fine grain size in polycrystal materials. Fine-grained materials have very good mechanical properties such as high strength at ambient temperature, superplasticity under appropriate deformation conditions and beneficial chemical properties [8, 9].

One could expect that using the ECAP process of aluminium bronzes the grain microstructure could be changed. However very high mechanical properties of aluminium bronzes at room temperature and at elevated

temperature could make difficult the ECAP deformation. In literature there is information about ECAP deformation only soft material such as aluminium, copper sometimes the low carbon steel [10, 11].

It was claimed that during ECAP pressing, the working pressure and load are relatively lower, however, for practical application, very severe friction appears during the ECAP processing. This makes the processing extremely difficult and could cause not uniform deformation in the cross section of extruded material. Recently more often the numerical method such as FEM has been applied to analyze the different metal forming processes. It could be very useful especially to analyze the strain distribution in ECAP process, however obtaining trustworthy results require very precise description of boundary condition and model material [12-16].

In ECAP the material is pressed by a ram through the channels in a die. The channels intersect at set angle Φ (Fig. 1). The magnitude of the strain depends on the size of angles Φ , Ψ and the friction conditions at pressed material/channel wall contact [17].

Mainly three deformation paths: A, B and C are used in ECAP (Fig. 2). In method A the sample is oriented identically in the successive passages whereby the deformation of the structure successively increases. If angle Ψ is equal to 0° the average deformation in a single passage is determined from the formula: $\varepsilon = \frac{2}{\sqrt{3}} \cos \Phi$. In order to determine the total deformation for n passages, the value for one passage should be multiplied by the number of passages. Obviously, the deformation is not uniform in the cross section because of friction. However, because of the complex state of strain, the distribution of strains cannot be explicitly determined.

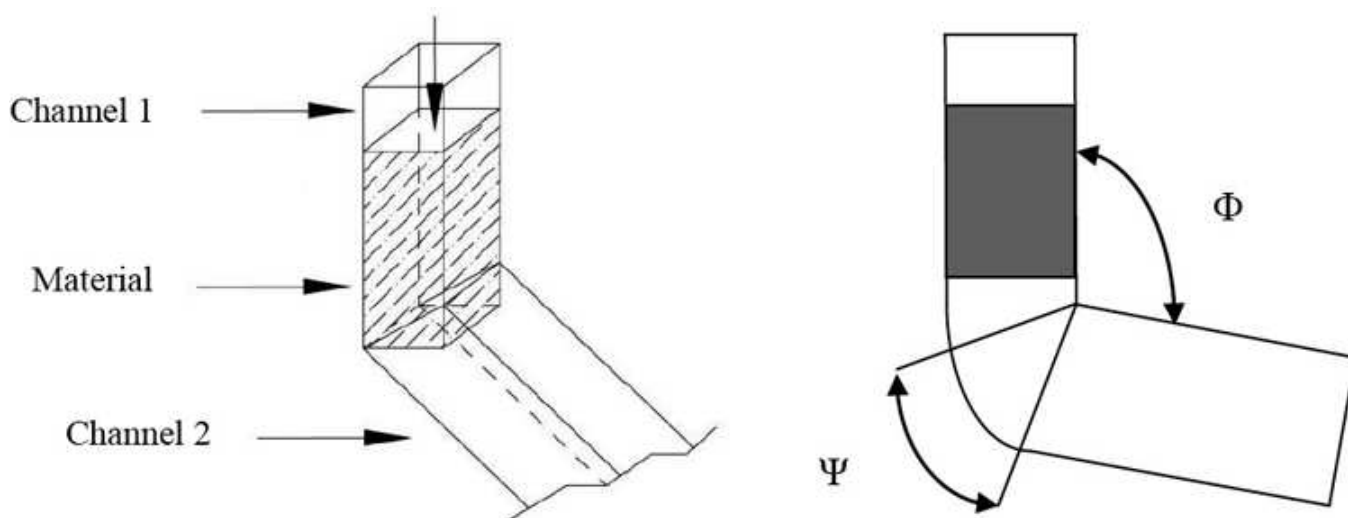


Fig. 1. Idea of ECAP

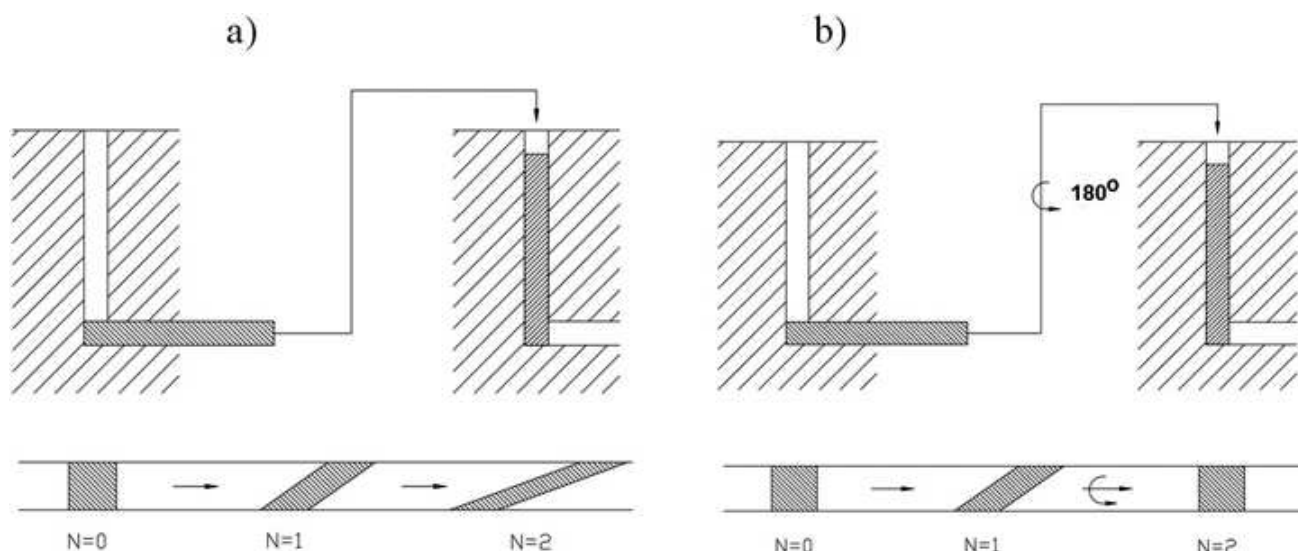


Fig. 2. Scheme of ECAP processes: a) method A – without rotation of samples and b) method C – with rotation of samples by 180°

For this purpose one should use, e.g., the finite element method. In method B, the sample after each strain cycle is rotated by 90°. Also in this case, the deformations in the successive cycles add up, but to a lesser degree than in method A. Deformation methods A and B cause very strong deformation of the microstructure due to the adding up of the strains in the successive cycles whereby the material quickly fails. Therefore method C, in which the sample is revolved by 180° around its axis, is most often used [18-20].

The aim of the research was to determine: the deformation condition of ECAP process of aluminium bronze BA1032, the strain distribution in sample through the cross section by FEM and research into structural phenomenon in aluminium bronze BA1032 deformed by ECAP. Therefore the maximum deformation temperature was set at 550°C since above this temperature recrystallization occurs, cancelling out the strain hardening effect. The presented research results should contribute not only to better control aluminium bronzes structure but also to significant advances in the field of ECAP deformation of high strength material.

The ECAP process analysis included:

- the design and construction of laboratory stands for forming of aluminium bronzes,
- the mathematical modelling of ECAP, aimed at determining deformation heterogeneity in the cross section of the sample,
- experiments on the real material.

2. Researched material

In the research the bronze BA1032 was used with following chemical composition.

TABLE 1
Chemical composition of aluminium BA1032

No.	sample	%Cu	%Al	%Fe	%Ni	%Mn	%Zn	%Pb
1.	BA1032	84.80	10.50	2.70	–	1.90	0.09	0.002

The manganese additions were to enhance the mechanical properties and abrasion resistance of the bronzes and the iron addition was to ensure their close-grained structure. The elements could be added only in small amounts permissible by the standards since if they were added in larger amounts, the corrosion resistance – an essential property of aluminium bronzes – would decrease.

The aluminium bronzes were gravity cast in the form of cylindrical ingots 205 mm in diameter, using the semi-continuous method. Then they were mechanically cut into 800 mm long sections, which were extruded the Hutmen S.A. Company into bars of ϕ 20 mm at temperature of 900°C on horizontal hydraulic presses. This is the simplest and most economical technology for the mass-production forming of aluminium copper alloys, available today.

The microstructures of the polished sections of plastically undeformed aluminium bronze BA1032 taken from the ingot are shown in Fig. 3.

The light grains are those of solid solution α seen against the background of dark eutectoid ($\alpha + \gamma_2$) being the result of the decomposition of phase β . Inside the grains and at their boundaries there are grey fine segregations of a phase rich in iron (the iron phase). Rosette-like segregations rich in iron are visible against phase α (Fig. 3). This is confirmed by SEM and EDS. The structural examinations showed that the hot extrusion of aluminium bronze BA1032 at a high temperature

of about 900°C causes strong phase refinement indicating intensive dynamic recrystallization and no secondary grain growth (Fig. 4).

In comparison with the ingot's structure, the initial structure of the bar is fine-grained, the segregations of phase α surrounding eutectoid $\alpha + \gamma_2$ are about 8 μm in

size. Against the background of phase α and the eutectoid, segregations rich in iron are visible. The latter are more spherical in comparison with the ones in the ingot (Fig. 3). The hardness of the initial material was about 240 HV1.

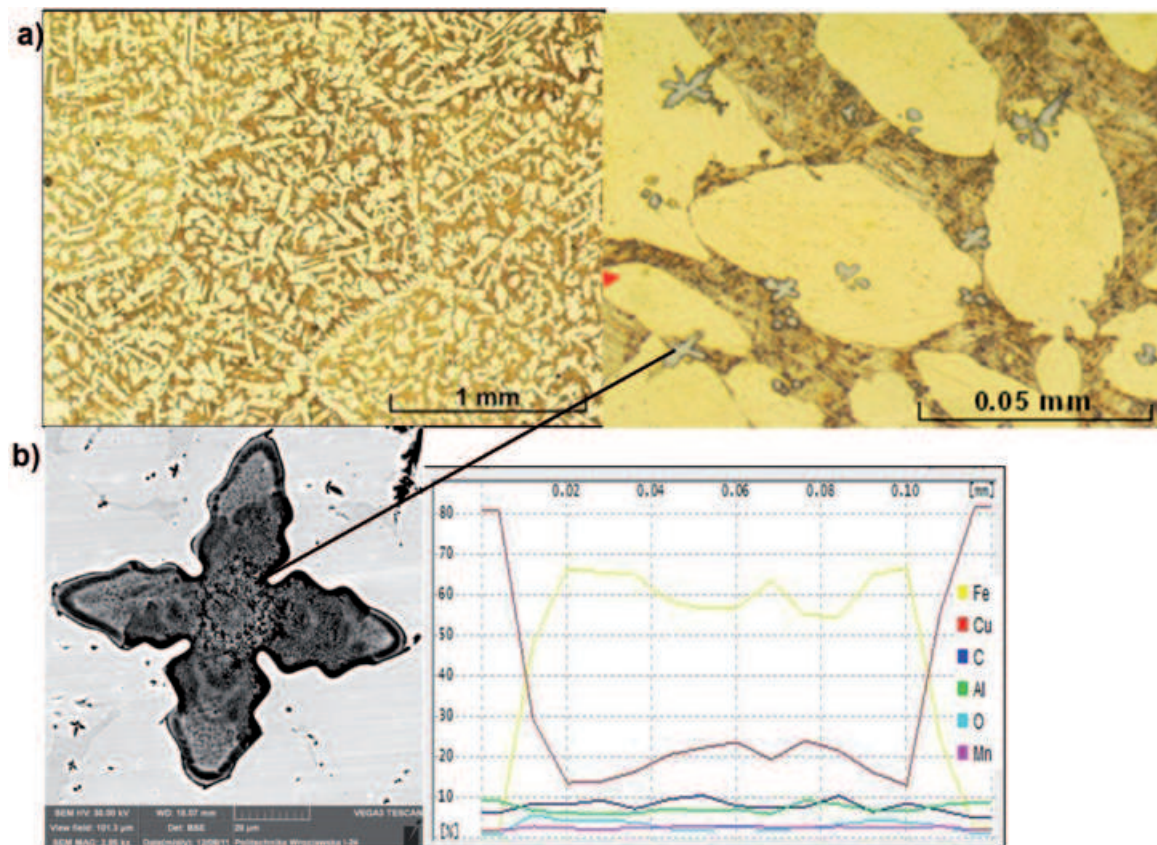


Fig. 3. Microstructure of BA1032: a) ingot after casting, b) rosette-like segregation rich in iron and results of X-ray analysis and image taken by BSE detector through the segregation

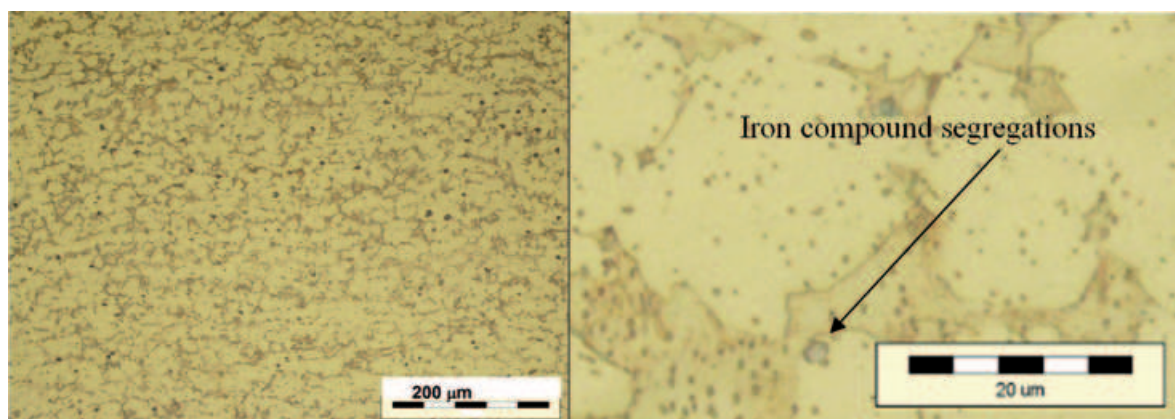


Fig. 4. Microstructures of aluminium bronze BA1032 after extrusion from bar (longitudinal section, etched condition), under different magnifications

3. Experiment

Description of test stand for ECAP

The test stand consisted of a mechanical press Tiratest 2300, equipped with a computer control system ensuring precise control in a wide range of strain rates, dies for ECAP and a regulated furnace.

The tested aluminium bronzes have a very high yield point and their strength is much higher than that of many low-carbon steels. Preliminary studies showed that it was not possible to test the materials at ambient temperature because the samples would crack. Therefore the maximum deformation temperature was set at 550°C since above this temperature recrystallization oc-

curs, cancelling out the strain hardening effect. The preliminary tests were carried out in dies at two different angles: $\Phi = 90^\circ$, 110° for cross sectional channel dimensions of 5×5 mm. The dies were made of hot-work tool steel WCL and consisted of an inlet channel, and outlet channel and 2×2 mm channel for a thermocouple measuring temperature inside the die. The die with a 5×5 mm channel had also five holes for erection bolts (Fig. 5). Since the outlet channel performs a calibration function it is essential to preserve the inlet channel dimensions in it. Otherwise, the samples would be curved (arc-shaped). In the investigated process the dies, the ram and the tested material were lubricated with graphite grease.

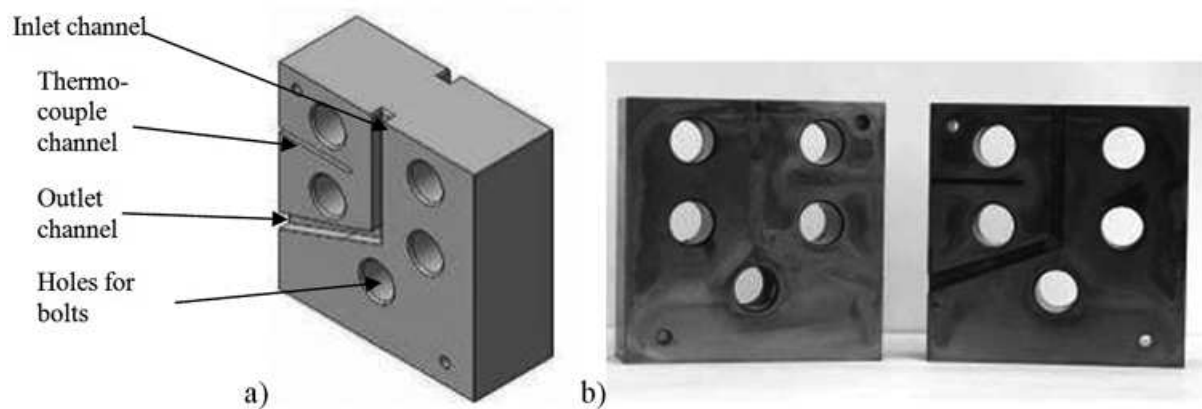


Fig. 5. ECAP die with 5×5 mm channel: a) die model made in CATIA, b) two-component die



Fig. 6. Sample deformed by ECAP at temperature below 350°C

Different extrusion temperatures and die angles were tried in preliminary tests. At temperatures below 350°C the samples were found to crack as a result of material shear (Fig. 6). Preliminary studies showed that in a temperature range of 400-500°C aluminium bronze in the form of a bar could be extruded only according to scheme C (rotation of the sample after each ECAP cycle) and at angle of 110°. The use of other ECAP schemes, in which deformation adds up in the successive cycles, would result in the cracking of the samples in the second cycle.

Conclusion of initial test is that the samples would no longer crack at a temperature of 400-500°C at die angle $\Phi = 110^\circ$. The next task was to build a stand enabling the extrusion of samples large enough for further processing. The stand which was built enabled the extrusion of 10.5×10.5 mm samples. The die consisted of two parts: an outer part and an inner part (Fig. 7). The inner part consisted of two parts forming a truncated cone with a flare angle of 10° ensuring that the extrusion

force pressed the two parts of the cone together. An inlet channel and an outlet channel were made in each of the parts in such a way that the two components when put together and placed in the casing (the die's outer part) formed a channel having the desired dimensions. This design makes it possible to use the ECAP force to press the cone to the casing. A hole was made in the casing to provide a free way out for the material extruded from the cone outlet channel. In addition, the dimensions of the casing outlet hole were such that flare angles Φ between the cone's inlet channel and outlet channel could be changed from 90 to 135°. The rate of extrusion was 0.2 mm/s.

The desired ECAP temperature was produced by a thermoregulator-controlled heater (Fig. 8) in which the whole die set would be placed. The process temperature was controlled by two thermocouples, one measuring the temperature of the tools and the other measuring the temperature of the air between the tools and the heater.

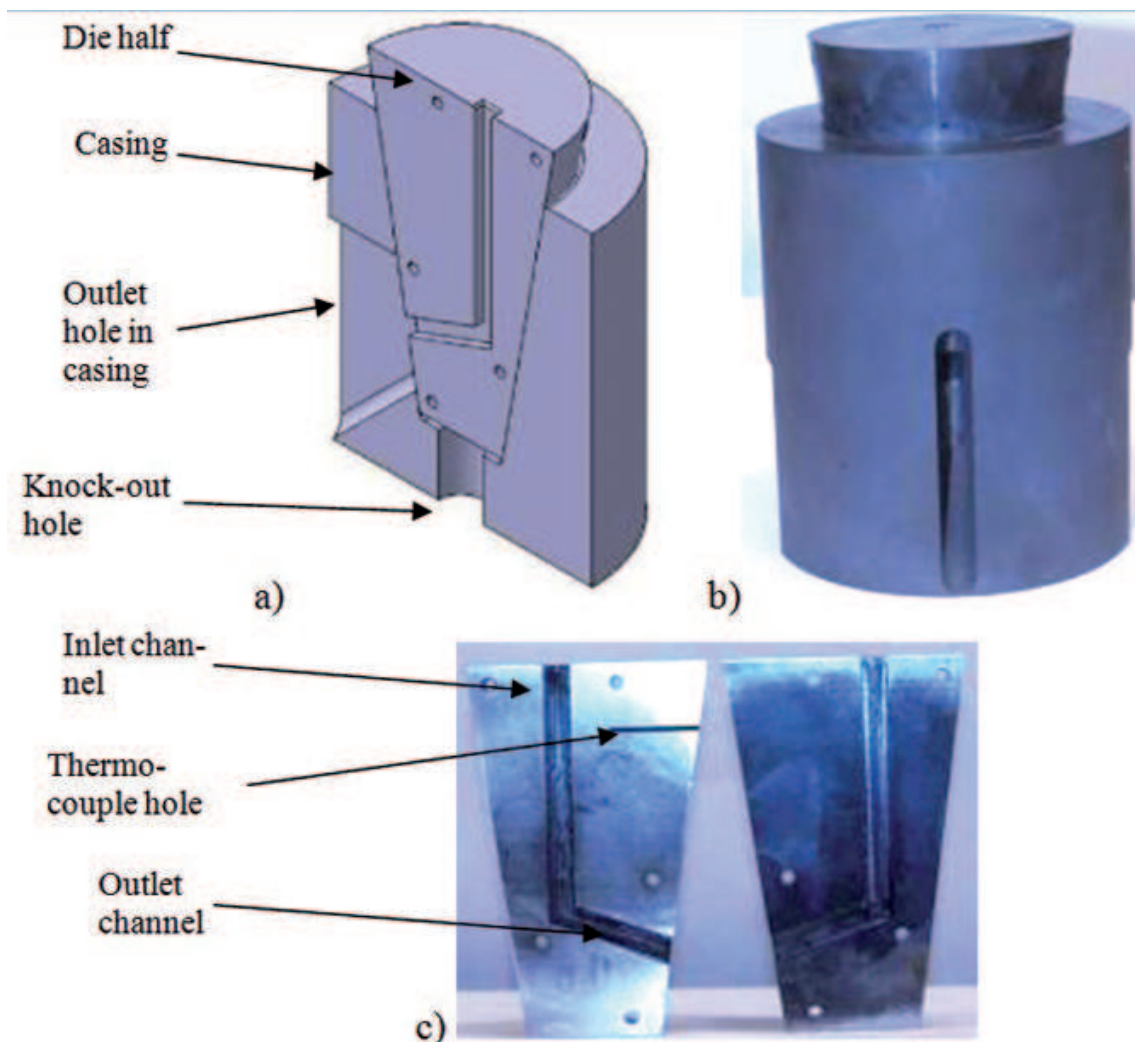


Fig. 7. ECAP die with 10.5×10.5 mm angular channel: a) view of ECAP cross section created in CATIA, b) die with casing c) die components forming cone with angular channel $\Phi = 110^\circ$

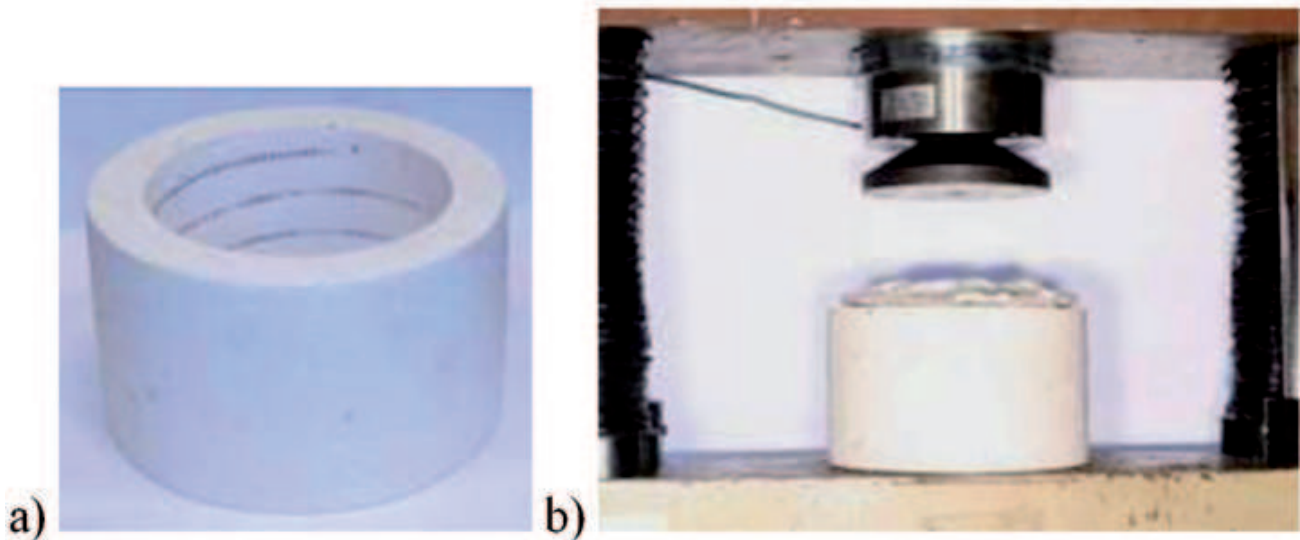


Fig. 8. Stand for ECAP tests: a) furnace and b) stand for hot ECAP tests on TiraTest press

Microhardness and EBSD research

Analysis of microhardness was carried out on the hardness testing machine LECO 100AT. The load 1000 g and 10 s of loading time were applied. The polishing and etching samples using Mi20Cu and Mi22Cu according to the norm PN-75/H-04512 were used. Average dimensions of the indents formed in the surface of test specimen are following: diagonal $80\ \mu\text{m}$ and side $60\ \mu\text{m}$. Taking into account the size of phase α (before deformation about $8\ \mu\text{m}$ in diameter and after deformation much lower) and the size of eutectoid which is much lower than phase α , the measured microhardness represents the average hardness of obtained structure.

In order to determine the degree of grain refinement in ECAP process the investigation was conducted with SEM_FEG "Inspect" combined with EBSD. The samples for the investigation were initially polished mechanically and that using ion beam with PIPS Precision Ion Polishing System. The field emission gun was at 20 KV and the spot size was 5.5 nm. TSL-OIM Data Collection system for the measurement process control and diffraction pattern indexing was used in the course of the investigation.

4. Numerical modelling of ECAP process

Computer simulations were run in order to determine strain heterogeneity in the cross section of the sample. A numerical plane-state-of-stress thermomechanical model was created for extrusion with sample rotation after each extrusion stage (C). The MSC.Marc Mentat 2009 computing package was used for the modelling. Flow stress-strain curves were determined through the

torsion test and derived in the numerical form for different strain values, strain rates, temperatures and materials. A hundred and eighty quad 4 elements were used for each sample to discretize the material being deformed. Automatic deformed grid remodelling with a change in the number and density distribution of elements, connected with element deformation and penetration into the tools, was employed. In the numerical channel test model all the tools, i.e. the ram and the forming die were assumed to be stiff. Boundary conditions similar to the ones which occur in the real process were assumed. Bilinear shear model SHEAR and the following heat exchange coefficients: specific heat = $0.92\ \text{kJ}/(\text{kgK})$ and thermal conductivity = $303.5\ \text{W}/(\text{mK})$ for the bronze and specific heat = $0.46\ \text{kJ}/(\text{kgK})$ and thermal conductivity = $15\ \text{W}/(\text{mK})$ for the steel tools (the ram and the die) were adopted. The linear velocity of the ram was $0.2\ \text{mm}/\text{s}$. Initially a constant friction coefficient value of 0.10 (determined by the ring test) for the particular tools was introduced. The mathematical process was verified with the extrusion forces determined in a real process and with the deformation of the grid superimposed prior to extrusion. The material flow obtained by FEM for the above conditions only slightly differed from the real one. The force level as a function of ram distance was more than 15% lower than in the real process. Therefore the coefficient of friction was increased to 0.15.

Figure 9 shows the distribution of total equivalent strain (the sum of the strains in the successive cycles; the strain increasing with each cycle) for method C. The results show that the largest strain heterogeneity exists in the first and third cycle. The largest strains occur in the sample's upper part while the smallest strains occur in its lower part.

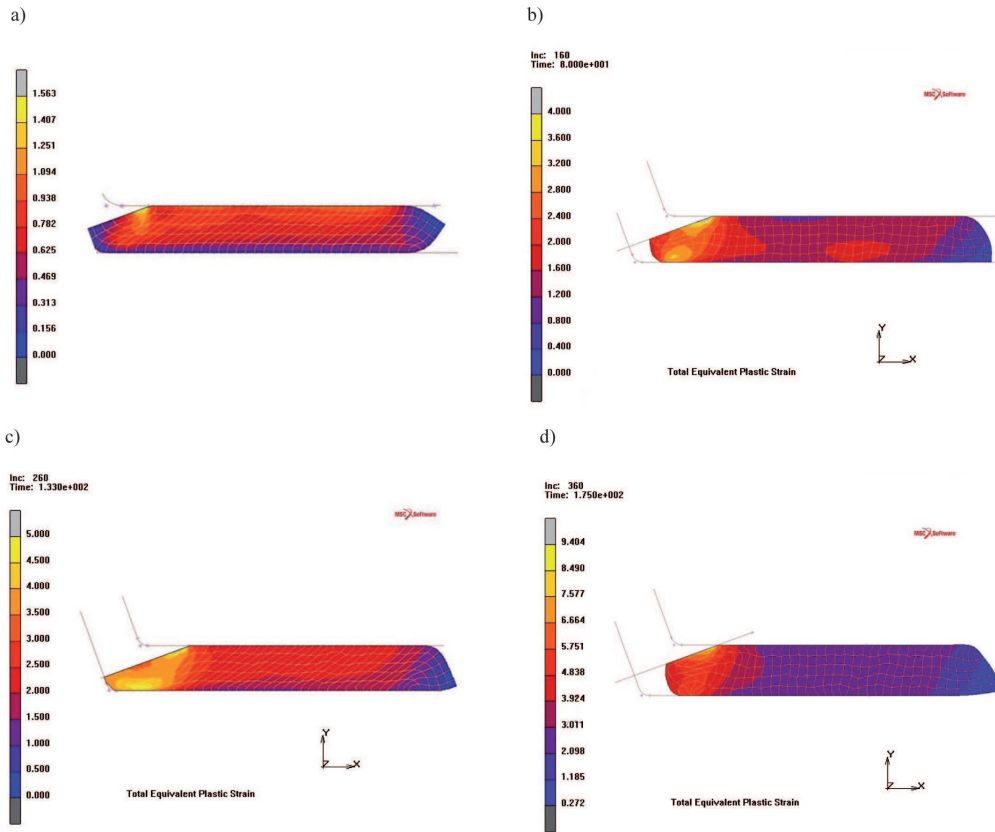


Fig. 9. Distribution of total equivalent plastic strain in successive extrusion cycles: a) after cycle 1, b) after cycle 2, c) after cycle 3 and d) after cycle 4

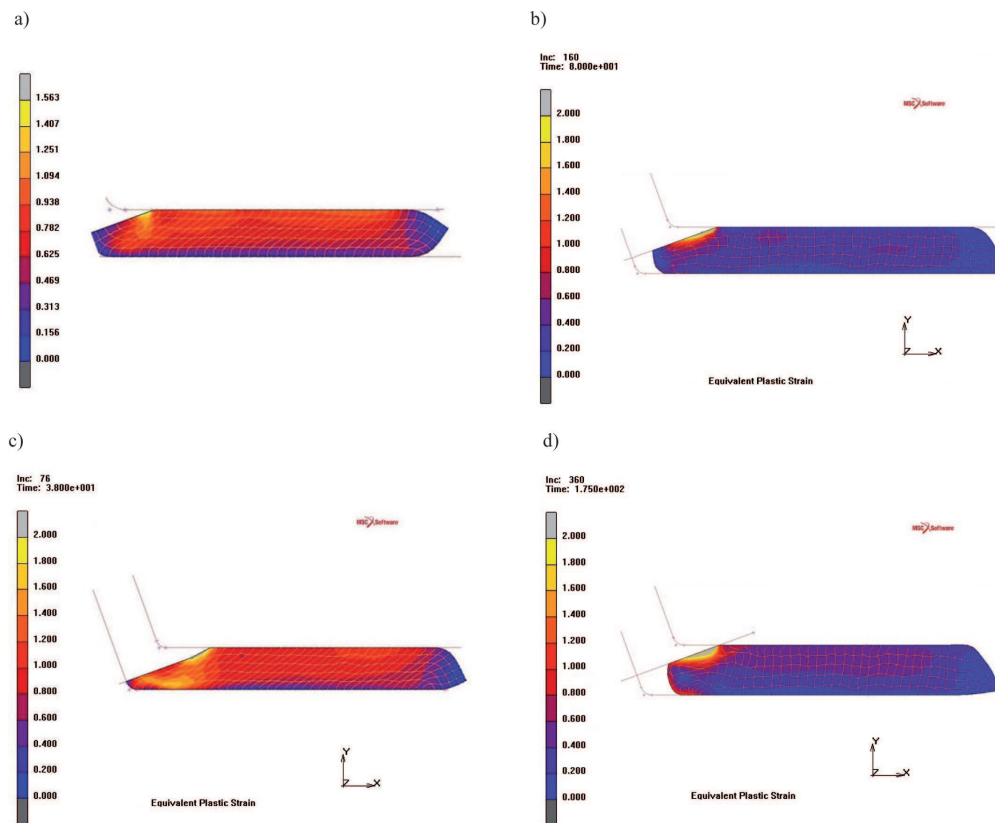


Fig. 10. Distribution of equivalent plastic strain in successive stages of extrusion: a) after cycle 1, b) after cycle 2, c) after cycle 3 and d) after cycle 4

If one examines only the strains in the successive cycles, it appears that as a result of the return deformation the sample almost resumes its initial shape (Fig. 10). This is clearly visible in the flow grids marked in the figures, which in even cycles nearly return to their initial square shape.

The strain distributions after 4 cycle are highly uniform. The difference between the largest strains occur in the sample's upper part and the smallest strains occur in its lower part is less than 1 for total equivalent plastic strain whereas for equivalent plastic strain is about 0,3 (Fig. 11). In cycle 1 and 3 even though extrusion along path C results in very high strain homogeneity, there is a very narrow (about 0.8 mm) layer in the lower part of the sample, which remains little deformed (Figs 9a and 9c).

5. Deformation of aluminium bronze BA1032 by ECAP method C

Aluminium bronze BA1032 in the form of a bar was extruded at a temperature of 400°C. Figure 11 shows a diagram of the extrusion force. Initially, the force increases to 17 kN and then it temporarily falls to a level of 7 kN. This is due to the pressing the previous ECAP cycle material situated at the intersection of the inlet and outlet channels in the die. Subsequently the force increases, reaching its maximum at about 70 kN. During this time, the upsetting of the charge material takes place and its extrusion begins. Then the force falls smoothly and continually as the length of the material situated in the inlet channel and its friction against the ECAP channel walls decreases.

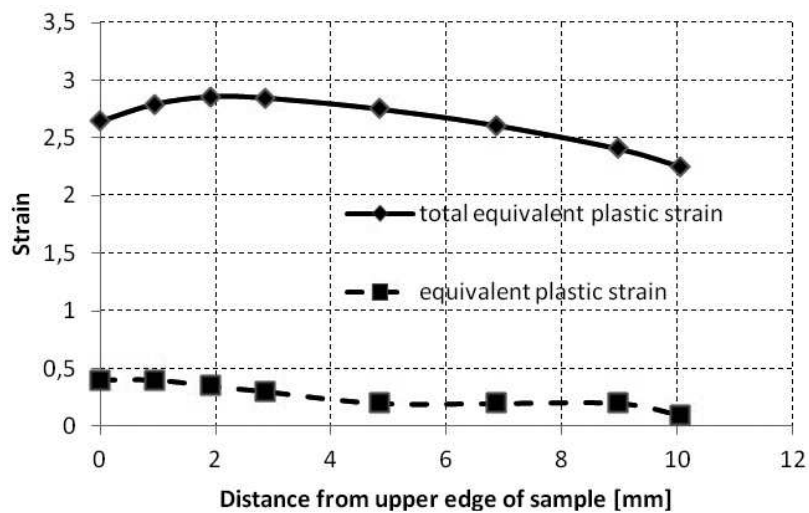


Fig. 11. Distribution of strains along sample thickness in cycle 4

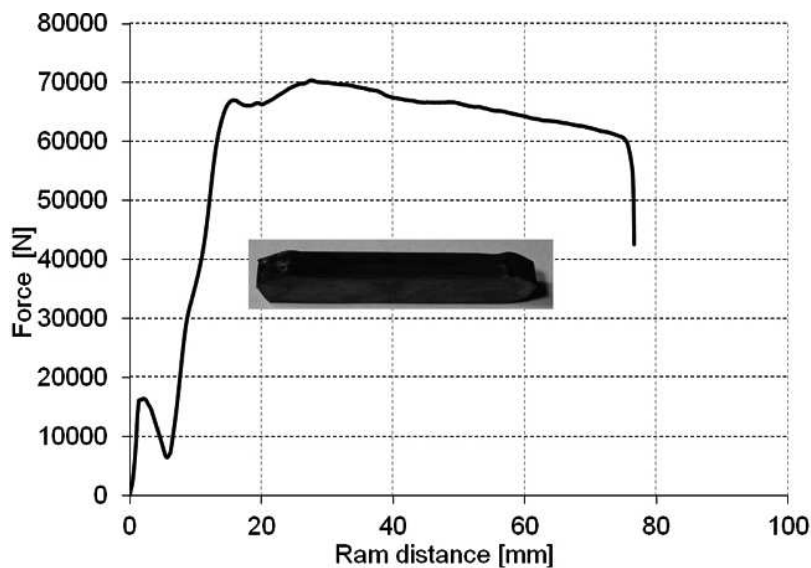


Fig. 12. Diagram of extrusion force for aluminium bronze BA1032 (bar) in first ECAP cycle at temperature of 400°C

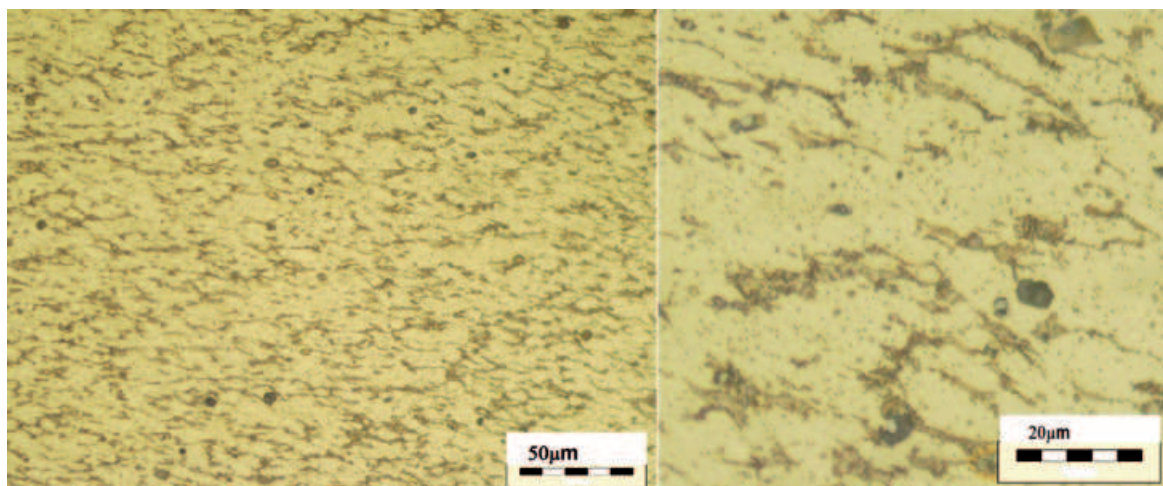


Fig. 13. Aluminium bronze BA1032 (bar) after first ECAP cycle

Figure 13 shows the microstructure in the middle part of the sample after the first ECAP cycle. It is difficult to determine the degree of deformation of the microstructure under low magnifications because the microstructure is very fine-grained. Only under higher magnifications the elongated eutectoid and phase α at an angle of 30–40° to the axis of the sample can be observed. During the first ECAP cycle the hardness of the bronze sharply increases to about 305 HV1 from initial hardness 240 HV1. As a result, the extrusion force in the second cycle increased to 100 kN.

If one examines the distribution of deformation in the cross section of the sample, one can notice that in its lower part there is a 0.8 mm thick layer which is little deformed while in its upper part, deformation nonuni-

formity is hard to find. Therefore it can be assumed that samples in the ECAP process are uniformly deformed along the whole sample width, except the ca 0.8 mm thick lower part of the sample. This is confirmed by the distribution of hardness along the sample's width (Fig. 14).

Since the sample in the second cycle was rotated by 180° around its axis in the die's inlet channel relative to the position of the sample in the previous ECAP cycle, its microstructure deformed in the first cycle should return to its original stated. This was, in fact, confirmed by structural examinations. The segregations of phase α have an equiaxial shape while eutectoid $\alpha + \gamma_2$ undergoes considerable refinement. The hardness of the aluminium bronze increases to about 320 HV (Fig. 15).

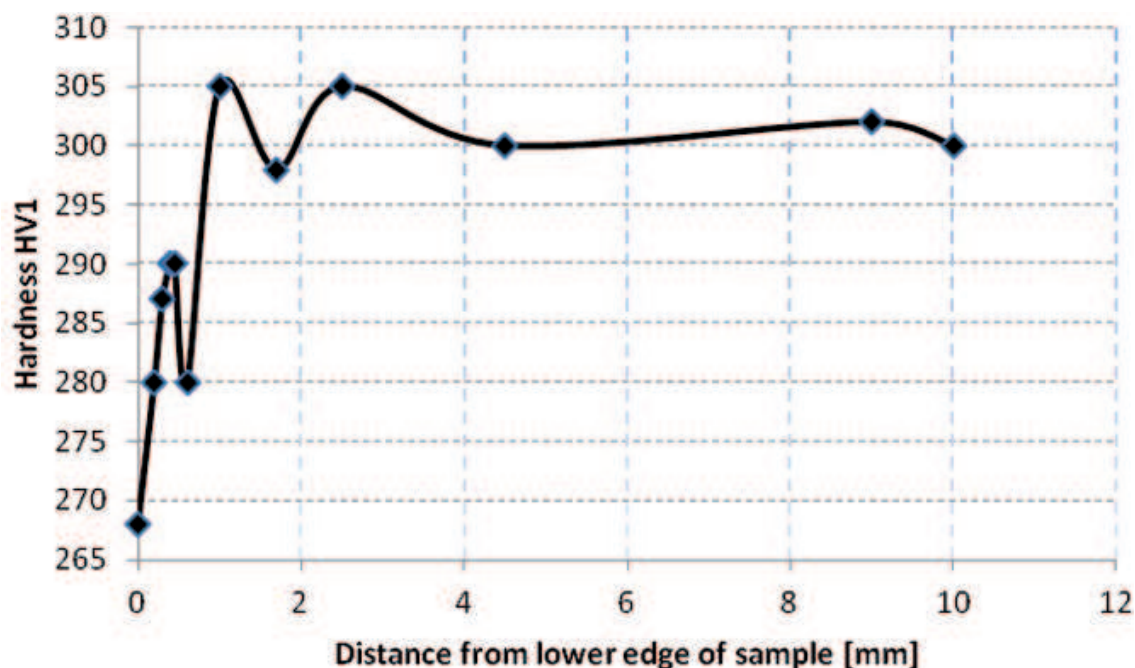


Fig. 14. Distribution of hardness in sample cross section after first ECAP cycle

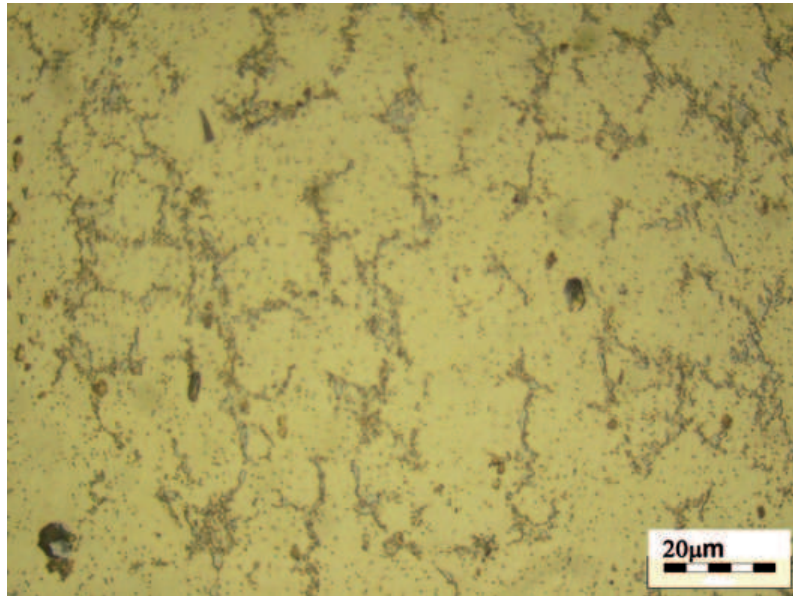


Fig. 15. Aluminium bronze BA1032 (bar) after second ECAP cycle

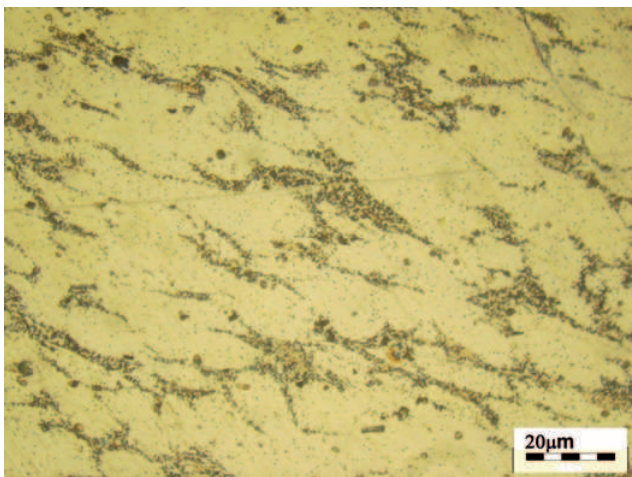


Fig. 16. Aluminium bronze BA1032 (bar) after third cycle of ECAP

In the third ECAP cycle, the eutectoid and phase α again elongate at an angle of 30-40° to the axis of the sample at extrusions forces similar to the ones in the previous cycles (Fig. 16). In the fourth (even) ECAP cycle the microstructure again returns to its original state (Fig. 17). The extrusion force and hardness are at similar levels as after cycle 2 and 3. In comparison with the initial microstructure, after four cycles neither the shape nor arrangement of phase α is changed, whereas the eutectoid is strongly refined.

In order to determine the degree of grain refinement, the samples were examined by EBSD. The initial structure consisted of equiaxed grains with an average misorientation angle of about 45°, however most orientations is within 30-60° with the peak located at 60°. Average grain size is 5 μm with a broad spread of grain

sizes around the mean value (Fig. 18a). An attempt was made to analyze the microstructure obtained after the fourth cycle of deformation, but it was found that the micro-structure becomes probably so strongly refined as

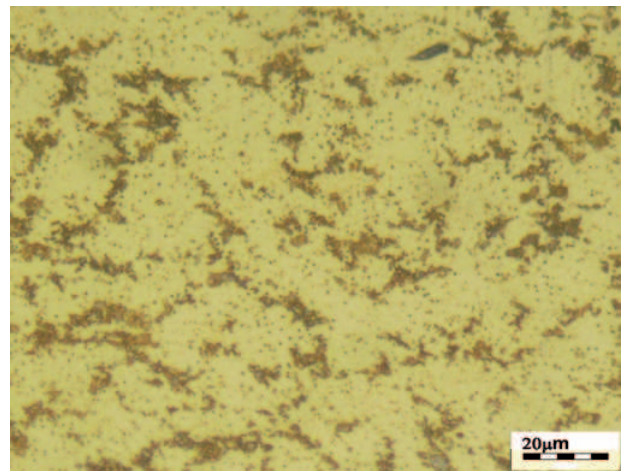


Fig. 17. Aluminium bronze BA1032 (bar) after fourth cycle of ECAP

a result of ECAP that the resolution of the available EBSD methods is insufficient to identify Kikuchi lines (Fig. 18b). The main problem with the results interpretation was connected with the diffraction pattern indexing of the severely deformed specimens. This could be connected to the diffraction band distortion or the formation of a new phase of unknown crystallographic structure. If it results from the first reason further TEM studies are needed to describe the phenomena associated with such a degree of structural refinement. This interpretation may be referred to as the working hypothesis.

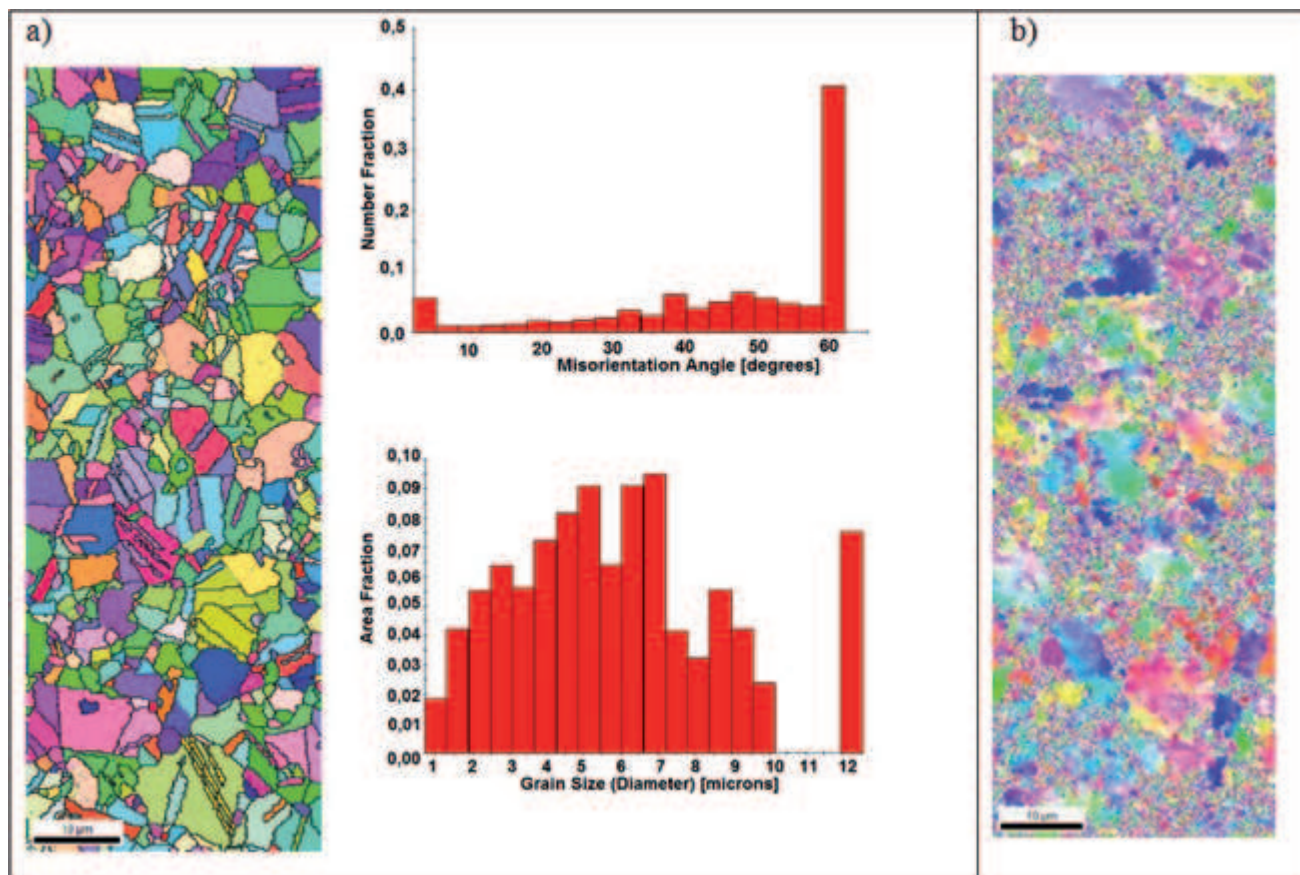


Fig. 18. Microstructure determined by EBSD a) initial b) after fourth cycle of deformation

6. Conclusions

The studies have indicated that it is possible to deform multiphase aluminium bronzes BA1032 in the ECAP process at a temperature of 400°C die angle $\Phi = 110^\circ$. The deformation of the bronzes at lower temperatures encounters some difficulties – cracks appear which make repeated ECAP impossible. The cracks appear on the top surface of the samples where it contacts the surface of the outlet channel. FEM simulations show that the largest plastic strains occur in this area.

Numerical simulations showed high deformation heterogeneity after the first cycle, which would be quickly removed in the second cycle by rotating the sample by 180°.

The proposed ECAP method of large plastic deformations as applied to the investigated aluminium bronzes makes it possible to obtain very strong refinement especially of eutectoid $\alpha + \gamma_2$.

In the case of aluminium bronze BA1032 in the form of a fine-grained bar, the microstructure becomes so strongly refined as a result of ECAP that the resolution of the available EBSD methods is insufficient to identify Kikuchi lines. This could be connected to the diffraction band distortion or the formation of a new

phase of unknown crystallographic structure. If it results from the first reason further TEM studies are needed to describe the phenomena associated with such a degree of structural refinement. This interpretation may be referred to as the working hypothesis.

REFERENCES

- [1] Z. Gronostajski, N. Misiołek, The effect of cyclic strain path on the properties and structure of CuAl10 aluminium bronze, *Journal of Materials Processing Technology* **155-156**, 1138-1143 (2004).
- [2] Z. Gronostajski, The deformation processing map for control of microstructure in CuAl9.2Fe3 aluminium bronze, *Journal of Materials Processing Technology* **125**, 119-124 (2002).
- [3] E.A. Culpán, G. Rose, Microstructural characterization of nickel aluminium bronze, *Journal of Material Science* **13**, 1647-1657 (1978).
- [4] K. Widancka, Effect of Boron on the Structure and Mechanical Properties of PM Fe-Si Compacts after through Vacuum Carburising, *Archives of Civil and Mechanical Engineering* **11**, 2, 469-477 (2011).
- [5] J. Iqbal, F. Ahmed, F. Hasan, Development of Microstructure in Silicon-Aluminum-Bronze, *Journal of Engineering & Applied Sciences* **3**, 47-53 (2008).

- [6] F. Filus, I. Schindler, G. Niewielski, D. Kuc, E. Hadasik, J. Fila, S. Lasek, T. Kubina, Elektro-chemical monitoring of static recrystallization, *Archives of Civil and Mechanical Engineering* **11**, 2, 277-283 (2011).
- [7] V.M. Segal, Materials processing by simple shear, *Materials Science and Engineering* **A197**, 157-164 (1995).
- [8] M. Richert, Strain-Stress Conditions of Shear Band Formation during CEC Processing on a New Machine with Control Back-Pressure, *Archives of Metallurgy and Materials* **55**, 2, 391-408 (2010).
- [9] W. Bochniak, A. Brzostowicz, Fabrication of Fine-Grained Flat Products by Continuous KoBo Method, *Archives of Metallurgy and Materials* **55**, 2, 587-560 (2010).
- [10] H. Paul, T. Baudin, F. Brisset, The Effect of the Strain Path and the Second Phase Particles on the Microstructure and the Texture Evolution of the AA3104 Alloy Processed by ECAP, *Archives of Metallurgy and Materials* **56**, 2, 245-261 (2011).
- [11] M. Kwapisz, M. Knapinski, H. Dyja, K. Laber, Analysis of the Effect of the Tool Shape on the Stress and Strain Distribution in the Alternate Extrusion and Multiaxial Compression Process, *Archives of Metallurgy and Materials* **56**, 2, 487-493 (2011).
- [12] T.T. Yu, P. Liu, Improved implementation of the extended finite element method for stress analysis around cracks, *Archives of Civil and Mechanical Engineering* **11**, 3, 787-805 (2011).
- [13] J. Ronda, A. Siwek, Modelling of laser welding process in the phase of keyhole formation, *Archives of Civil and Mechanical Engineering* **11**, 3, 739-752 (2011).
- [14] M. Pietrzyk, Ł. Madej, Ł. Rauch, R. Gołab, Multiscale modeling of microstructure evolution during laminar cooling of hot rolled DP steels, *Archives of Civil and Mechanical Engineering* **10**, 4, 57-67 (2010).
- [15] D. Kuc, J. Gawad, Modelling of Microstructure Changes during Hot Deformation using Cellular Automata, *Archives of Metallurgy and Materials* **56**, 2, 423-432, (2011).
- [16] D. Szeliga, R. Kuziak, V. Pidvysotsky, M. Pietrzyk, Rheological model of Cu based alloys accounting for the preheating prior to deformation, *Archives of Civil and Mechanical Engineering* **11**, 2, 451-467 (2011).
- [17] Y. Yoshinori, J. Wang, Z. Horita, M. Nemoto, T.G. Langdon, Principle of equal-channel angular pressing for the processing of ultra-fine grained materials, *Scripta Materialia* **35**, 2, 143-146 (1996).
- [18] L. Olejnik, A. Rosochowski, Methods of fabricating metals for nano-technology, *Bulletin of Polish Academy of Science, Technical Science* **53**, 4, 413-423 (2005).
- [19] A. Rosochowski, L. Olejnik, Numerical and physical modelling of plastic deformation in 2-turn equal channel angular extrusion, *Journal of Materials Processing Technology* **125-126**, 309-316 (2002).
- [20] A. Habibi, M. Ketabchi, M. Eskandarzadeh, Nano-grained pure copper with high-strength and high-conductivity produced by equal channel angular rolling process, *Journal of Materials Processing Technology* **211**, 1085-1090 (2011).